A&A 403, 1023–1029 (2003)
DOI: 10.1051/0004-6361:20030498

Astronomy & Astrophysics

Estimation of the mass loss, opening angle and mass of Be circumstellar disks from Brγ continuum emission and interferometric measurements

Ph. Stee⋆

Observatoire de la Côte d'Azur, Département FRESNEL, CNRS UMR 6528, Site de Grasse-Roquevignon, Avenue Copernic, 06130 Grasse, France

Received 2 December 2002 / Accepted 13 March 2003

Abstract. Using the SIMECA code developed by Stee & Araùjo (1994); Stee et al. (1995) for Be stars we obtain a correlation between the mass loss rates $\dot{M}$ and the Brγ continuum luminosity as a function of the opening angle of the disk. We show that this correlation is similar to those obtained by Scuderi et al. (1998) for O-B supergiants. We found that the wind density at the base of the photosphere, from a sample of 8 Be stars, lies between 10^{-13} and 10^{-12} g cm^{-3}. We also present a relationship between the mass of the circumstellar disk and the 2.16 μm flux. Finally we emphasize how interferometric measurements can help to estimate the wind density and we present a sample of 16 Be stars with predicted visibilities that can be observed with the VLTI.

Key words. stars: emission line, Be – stars: winds, outflows – technique: interferometric

1. Introduction

In a recent paper, Stee & Bittar (2001, hereafter SB) found that the near-IR emission both in the Brγ line and the nearby continuum originates from a very extended regions can be twice the size of the Hα-emiting region, i.e. up to 40 stellar radii. In that paper they also study the influence of the $m1$ parameter which describes the variation of the mass flux from the pole to the equator according to:

$$\phi(\theta) = \phi_{\rm pole} + \left[\left(\phi_{\rm eq.} - \phi_{\rm pole}\right)\sin^{m1}(\theta)\right] \quad (1)$$

where θ is the stellar colatitude. Since we assume that the physics of the polar regions is represented by a CAK-type stellar wind model (Castor et al. 1975), we introduce Eq. (1) in order to obtain solutions for all stellar latitudes. For $\theta = 0$ we consider the polar mass flux whereas equatorial values are obtained for $\theta = 90$. The disk is very flat for $m1 = 1000$ and forms a more or less ellipsoidal envelope for $m1 = 0.1$. They found that the envelope contribution in the line increases as the envelope becomes more and more ellipsoidal (lower $m1$). At the same time, the stellar contribution decreases from a very flat envelope to a more ellipsoidal one due to an increase in the absorption of the stellar continuum from the circumstellar envelope. Both effects tend to decrease the ratio of stellar/envelope continuum for more ellipsoidal geometries. They also notice that the envelope contribution in the Brγ line increases when the envelope becomes more "disk-like", unlike the envelope contribution in the Hα and Hβ lines, which decreases. Finally they found that the total flux decreases for flatter envelopes, i.e. for large $m1$ values. In the present paper we would like to investigate how the envelope's shape can be related to the stellar mass loss, the mass of the disk and if it is possible to use the Brγ continuum luminosity to deduce the disk geometry. Moreover, thanks to the forthcoming VLTI, we will also show that it is possible to estimate the wind density from visibility measurements. In Sect. 2 we will present the relationship between the $m1$ parameter used in SB and the disk opening angle. Section 3 presents the basic assumptions used in the SIMECA code. The opening angle-2.16 μm magnitude relation is presented in Sect. 4 and the mass loss rate and mass of the disk-2.16 μm flux correlation are given in Sect. 5. We discuss and compare our results with previous studies and finally the last section describes how interferometric measurements can help, knowing the K magnitude, to estimate the mass loss and the disk opening angle.

2. Relationship between the m1 parameter and the disk opening angle

As described in the introduction, the $m1$ parameter is a free parameter that describes the variation of the mass flux from the pole to the equator according to Eq. (1). In order to compare our results with previous studies, such as from Waters & Lamers (1987), we have calculated the corresponding disk opening angle, defined as the geometrical region where half of the polar mass flux originates. Thus, as shown in Fig. 1,

⋆ e-mail: Philippe.Stee@obs-azur.fr

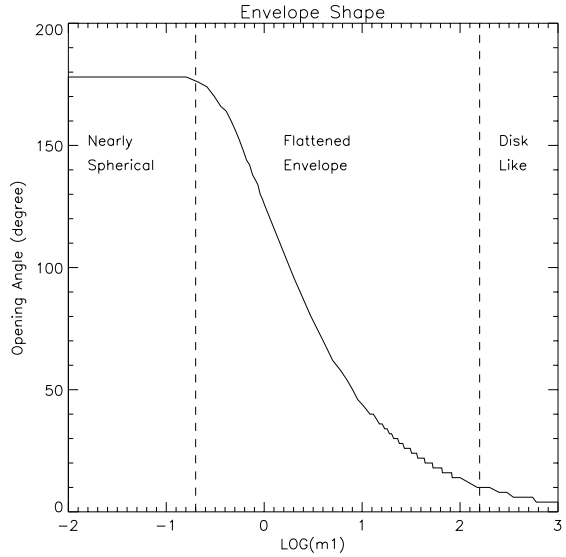

Fig. 1. Relationship between the free parameter $m1$ and the disk opening angle in degree (180° corresponds to a spherical circumstellar envelope).

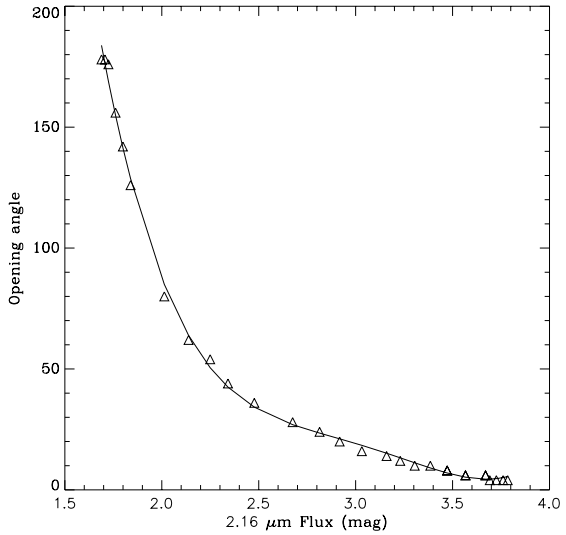

Fig. 2. Relationship between the disk opening angle in degree and the 2.16 μm flux (in magnitude).

we obtain very thin disk (i.e. 4°) such as disks produced by the Wind Compressed Disk (WCD) models (Bjorkman & Cassinelli 1993) for $m1 = 1000$ up to nearly spherical envelopes (i.e. 178°) for $m1 = 0.01$.

3. The SIMECA code

The SIMECA code is able to compute classical observables, i.e. spectroscopic and photometric ones but also intensity maps in Balmer lines and in the continuum. It is also possible to obtain theoretical visibility curves which can be directly compared to high angular resolution data. For this study, we have used SIMECA in order to compute the Brγ continuum luminosity at 2.16 μm as a function of the disk opening angle. The main hypothesis of this code is that the envelope is axi-symmetric with respect to the rotational axis. No meridian circulation is allowed. We assume that the physics of the polar regions is well represented by a CAK-type stellar wind model (Castor et al. 1975). The solutions for all stellar latitudes are obtained by introducing a parametrized model (the $m1$ parameter) that can be constrained by spectrally-resolved interferometric data. The inner equatorial region is dominated by Keplerian rotation.

In order to take into account the 7–4 levels radiative transition to reproduce the Brγ line profile at 2.16 μm, we consider hydrogen atoms with seven bound levels. The ionization-excitation equations are solved for an envelope modeled in a 170*90*71 cube. Since the final population of atomic levels are strongly NLTE distributed, we start with the LTE populations for each level, we then compute the escape probability of each transition which allows us to obtain up-dated populations, and we iterate until convergence. The convergence is quite fast (about ten iterations) and stable within an effective temperature of the central star in the range $10\,000 < T_{\rm eff} < 40\,000$. The basic equations of the SIMECA code are given in detail in SB.

In SIMECA the envelope temperature follows:

$$T(r) \propto \frac{T_{\rm eff}}{r^{\frac{1}{2}}} \tag{2}$$

where r is the distance from the central star in unit of stellar radius.

The density distribution is given by the equation of mass conservation:

$$\rho(r,\theta) = \frac{\Phi(\theta)}{\left(\frac{r}{R}\right)^2 v_r(r,\theta)}, \tag{3}$$

where $v_r(r,\theta)$ is the expansion velocity field given by:

$$v_r(r,\theta) = V_{\rm o}(\theta) + [V_\infty(\theta) - V_{\rm o}(\theta)]\left(1 - \frac{R}{r}\right)^\gamma, \tag{4}$$

with

$$V_{\rm o}(\theta) = \frac{\Phi(\theta)}{\rho_0} = \frac{\Phi_{\rm pole}\left[1 + (C1-1)\sin^{m1}(\theta)\right]}{\rho_0}. \tag{5}$$

$V_\infty(\theta)$ is the terminal velocity and R the stellar radius. C1, the equatorial and polar mass flux ration is typically between 10^1 and 10^4 (Lamers & Waters 1987) thus we used in this study $C1 = 30$. We also used a "γ-law" with $\gamma = 0.86$ which is a typical value for early Be stars (Poe & Friend 1986; Araújo & Freitas Pacheco 1989; Owocki et al. 1994). These values were also used with succes for the modeling of the "Classical" Be star γ Cas in Stee et al. (1995) and unless using very unusual values for Be stars must have a negligeable influence on the results presented in this paper. The parameter ρ_0 corresponds to the density at the base of the stellar photosphere. We will call it "wind density" in the following. More details about the basic equations used in SIMECA can be found in Stee et al. (1995).

4. Opening angle-2.16 μm magnitude relation

In Fig. 2 we plotted the relation between the disk opening angle and the 2.16 μm flux. As found by SB, the 2.16 μm magnitude

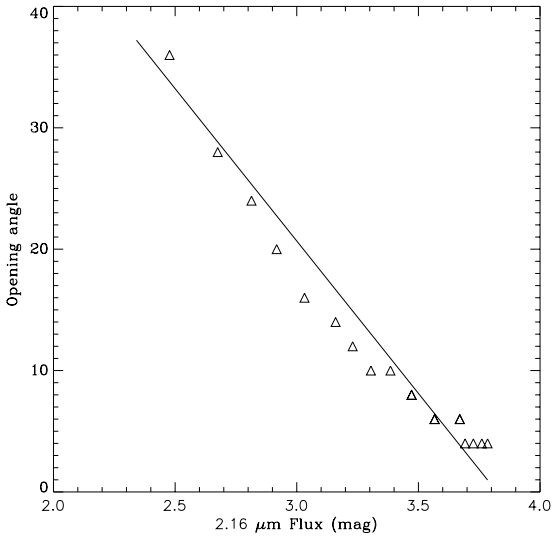

Fig. 3. Zoom on the relationship between the disk opening angle (from 0 to 40°) and the 2.16 μm flux (in magnitude).

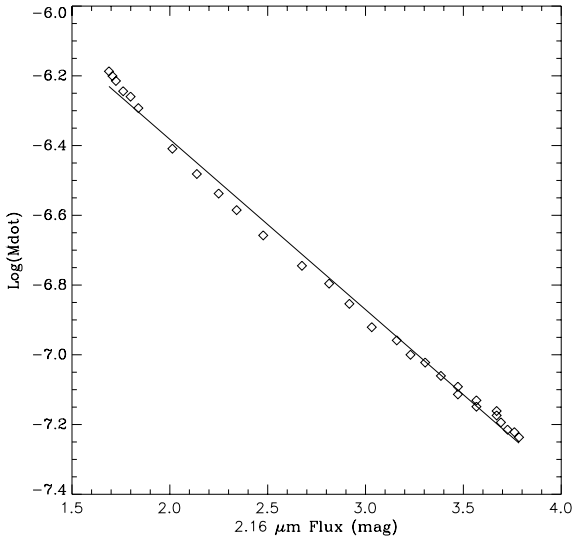

Fig. 4. Relationship between logarithm of the mass loss of the star and the 2.16 μm flux (in magnitude).

increases for flatter envelopes, i.e. for large $m1$ values which is simply due to a decrease of the total amount of gas that produce the Brγ continuum. Between 0 and 50° the 2.16 μm magnitude increase from 2.25 to 3.8, i.e gains 1.55 mag whereas between 50 and 180° it change by only 0.55 mag. It means that the Brγ continuum emission is very sensitive to the disk opening angle for "intermediate" disk size, i.e for disks between 0 and 50° of opening angle. Since the continuum emission originates mostly from the equatorial regions, the luminosity is only slowly increasing after 50°. It means that even if the gas is sphericaly distributed around the central star the Brγ continuum emission remains confined in the equatorial plane. This effect was already outlined in the paper by Stee & Araújo (1994) and is mainly due to the fact that the population of atomic levels strongly depends on the stellar latitude through the escape probability dependence. We found that the computed populations globally and rapidly decrease from the equator to the pole but most of the hydrogen atoms remain in the fundamental state. Thus the Brγ continuum as well as the Hα, Hβ and Brγlines originate from the equatorial regions.

It may explain why Yudin (2001), who present the results of statistical analyses of a sample of 627 Be stars found no correlation between the intrinsic polarization and the $E(V-L)$ excess: the largest IR excess may originate from Be disks with very different opening angles, i.e. between 50 and 180°, without major changes for the IR magnitudes but with large changes in the intrinsic polarizations from star to star.

In Fig. 3 we present a "zoom" between 0 and 40° which clearly shows a linear relation between the opening angle and the 2.16 μm magnitude which follows:

$$\theta = -25.1F + 96 \quad (6)$$

where θ is the opening angle of the disk in degree and F is the 2.16 μm flux (in magnitude). We can notice that for very small opening angles, we obtain different 2.16 μm flux values for the same opening angle. This is due to our opening angle definition which corresponds to the geometrical region where half of the polar mass flux originates. Thus for very large $m1$ values, i.e. very small opening angles, this criterion is not sensitive enough and it is not possible to distinguish between different opening angles.

5. $\dot{M}$–F correlation

Following the study by Scuderi et al. (1998) who obtain a $\dot{M}$–L relationship for O and B supergiants using Very Large Array (VLA) radio observations correlation we propose to study the possible correlation between $\dot{M}$ and the 2.16 μm flux (F). In Fig. 4 we have plotted $\dot{M}$–F where each point corresponds to one $m1$ value, i.e. one opening angle. The 2.16 μm flux is correlated to the mass loss rate following the relation:

$$\log(\dot{M}) = -0.48F - 5.40. \quad (7)$$

If the 2.16 μm *luminosity* is plotted instead of the 2.16 μm magnitude (see Fig. 5), Eq. (9) becomes:

$$\log(\dot{M}) = 1.22 \log(L_{\mathrm{Br}\gamma}) \quad (8)$$

which is very close to the relation $\dot{M}$-L obtained by Scuderi et al. (1998) for O and B supergiants, i.e. $\log(\dot{M}) = 1.22\ \log(L_{\mathrm{Br}\gamma}) \pm 0.30$ from VLA observations of 12 sources. This is not surprizing since the 2.16 μm emission from Be stars is of thermal origin, i.e. free-free and free-bound radiation produced in the outer parts of the wind as for O and B supergiants.

For each model we have also computed the total mass of the disk. Again, we found a clear correlation between the mass of the disk and the 2.16 μm flux. As for the $\dot{M}$–F relation, each point corresponds to one $m1$ value, i.e. one opening angle. From Fig. 6 we can see that the mass of the disk follows:

$$\log(M_{\mathrm{disk}}) = -0.37F - 7.54. \quad (9)$$

6. Discussion and comparison with previous studies

In order to compare our theoretical results using SIMECA with previous studies, we have computed the IR mass loss, the disk

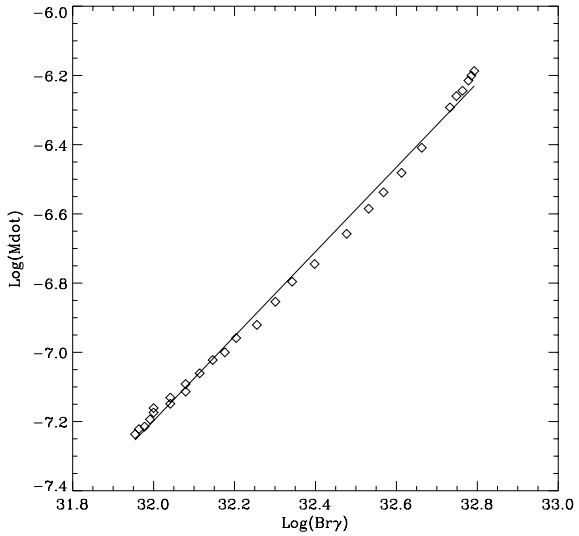

Fig. 5. Relationship between logarithm of the mass loss of the star and the logarithm of the Brγ continuum emission. This correlation is of the same nature has found by Scuderi et al. (1998) for O-B supergiants.

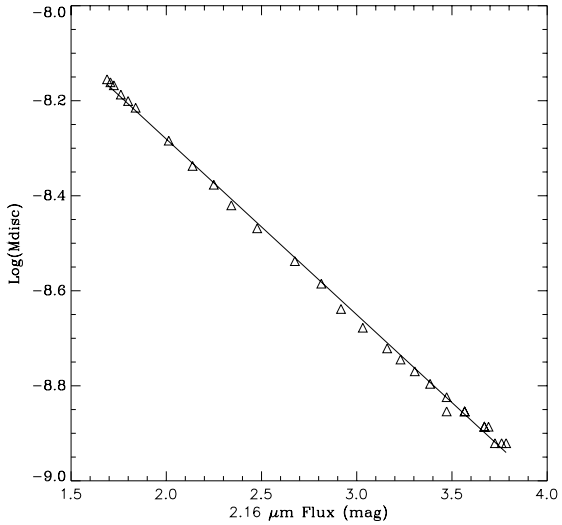

Fig. 6. Relationship between logarithm of the mass of the circumstellar disk and the 2.16 μm flux (in magnitude).

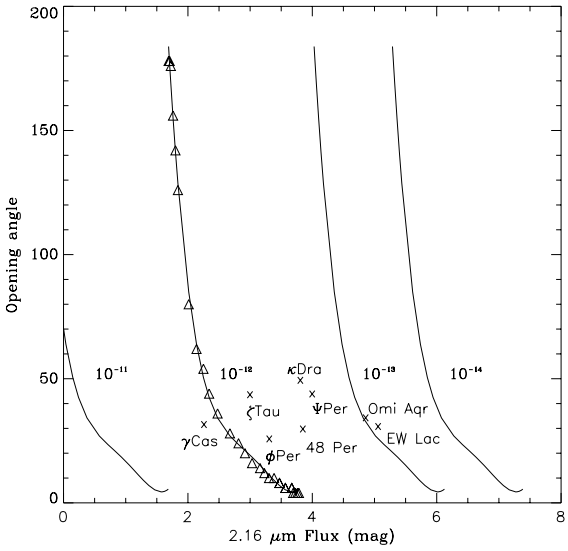

Fig. 7. Relationship between the disk opening angle in degree and the 2.16 μm flux (in magnitude) for different densities at the base of the stellar photosphere indicated on the plot (in g cm^{-3}). We have overplotted the opening angles and the 2.16 μm flux determined by Waters et al. (1987).

opening angle and the mass of the disk for 8 Be stars selected by Rinehart et al. (1999). The estimation of the IR mass loss and the disk opening angle was taken from Waters et al. (1987) whereas the mass of the disk was taken from Rinehart et al. (1999).

Our mass loss rate determinations are, as a whole, larger compared to the Waters et al. estimations except for EW Lac and ψ Per which are found to be smaller by a factor of 3. We also obtain larger mass of the circumstellar disk compared to Rinehart et al. (1999). Nevertheless, in both cases their estimations were made using very simple models. In Rinehart et al. (1999), they assumed that the IR emission arises from an extended stellar envelope around the star which is flattened into an oblate spheroidal disk, with a semiminor/semimajor axis ratio of ~1/10. The density and temperature within the envelope are assumed to be uniform. In Waters et al. (1987) they used a very simple disk geometry to interpret the observed far-IR fluxes. The disk is supposed to be isothermal, viewed pole-on for all stars with a given opening angle and radius. The density in the disk follows a power law with a density parameter that is adjusted to fit observed curves of growth.

Nevertheless, we may wonder if our results are representative of all the Be stars since our calculations were done for one effective temperature, i.e 25 000 K and a given wind density, i.e. 2×10^{-12} g cm^{-3}. The answer comes from the study by SB which shows that the near-IR continuum originates mainly from free-free and free-bound transitions. Since the envelope is completely ionized between 16 000 and 40 000 K, the continuum emission is not very sensitive to the temperature within the disk. Thus our results remain valid within the given temperature range. On the opposite, our results are very sensitive to the wind density. The wind density usually lies between 10^{-14} and 10^{-11} (Gehrz et al. 1974; Dachs et al. 1988; Hony et al. 2000). Thus we have plotted in Fig. 7 the relation between the opening angle and 2.16 μm flux for densities within this range. We obtain the same curves as Fig. 2 but shifted by −2.1, 2.34 and 3.6 mag, respectively for the densities 10^{-11}; 10^{-13} and 10^{-14} g cm^{-3}. The corresponding $\dot{M}$–F relationship are plotted in Fig. 8. Again, a density change produces a simple shift of the correlation curve obtained for $\rho_0 = 10^{-12}$ plotted in Fig. 4.

We also found from Table 1 that stars with large IR magnitudes must have a very thin disk, i.e. an opening angle of a few degrees (see for instance ψ Per or Omi Aqr). Nevertheless, all the listed stars are classified as "Shell-stars", except for EW Lac. A shell profile is usually due to a large colum depth of circumstellar material that causes a partial obscuring of the stellar disk and thus a shell absorption. It may be a clear indication that the disks around the central stars are not geometrically very thin. For instance, from Fig. 7, it is clear that, if you take the 2.16 μm magnitude of the 8 Be stars from Rinehart et al. (1999) and the corresponding disk opening angle from

Table 1. Mass of the disc from Rinehart et al. (1999), mass loss and disc opening angle from Waters et al. (1987) compared to SIMECA values.

star	2.2 μm Flux (mag)	$\log(\dot{M}_{IR})$ ($M_\odot$/year)	$M_{\rm disk}$ (10^{-10} $M_\odot$)	θ (degree)
ψ Per	3.94	–6.9	9.3	42.5
SIMECA		–7.3	10.0	∼1
η Tau	2.96	–	0.93	–
SIMECA		–6.8	22.9	20.0
ζ Tau	2.94	–7.6	8.3	42.2
SIMECA		–6.8	23.4	22.0
48 Per	3.79	–7.9	3.7	28.4
SIMECA		–7.2	11.2	∼2
ϕ Per	3.25	–7.3	17.6	24.4
SIMECA		–7.0	18.1	14.0
γ Cas	2.2	–6.9	81.4	30.2
SIMECA		–6.6	43.6	54.0
Omi Aqr	4.8	–8.8	0.25	32.9
SIMECA		–7.8	4.2	∼1
EW Lac	5.0	–7.6	3.2	29.4
SIMECA		–8.1	2.6	∼1
κ Dra	3.75	–7.9	1.2	48.0
SIMECA		–7.2	11.4	∼2

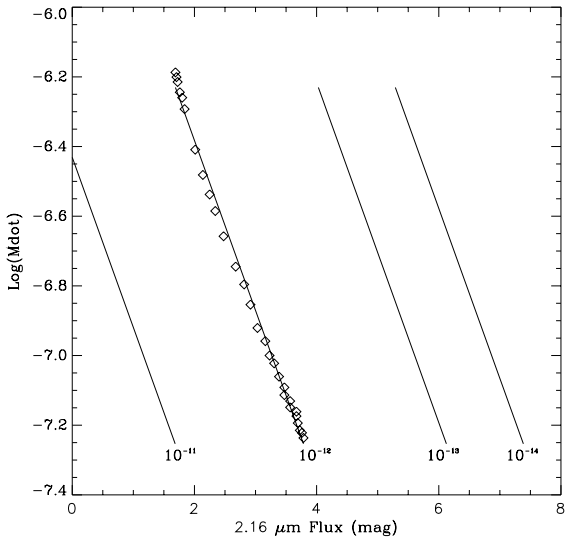

Fig. 8. Relationship between logarithm of the mass loss of the star and the 2.16 μm flux (in magnitude) for different densities at the base of the stellar photosphere indicated on the plot (in g cm^{-3}).

Waters et al. (1987), the density at the base of the photosphere lies between 10^{-12} and 10^{-13} g cm^{-3}. This is true for all the Be stars in our sample, excepted for γ Cas that appears to have a more massive disk, i.e. larger than 10^{-12} g cm^{-3}. Thus, if you want to estimate the disk opening angle you have to know the wind density and vice versa, i.e. it may be possible to estimate the wind density, knowing the K magnitude and the opening angle of the disk thanks to interferometric measurements. This will be discussed in the next section.

Another important issue is that the Waters et al. (1987) models do not allow solutions for disks with opening angles larger than 50°, which is not the case for our SIMECA models. Unfortunately, we recall that, as already mentioned by Quirrenbach et al. (1997), interferometric observations do not allow a separate determination of the inclination and the thickness of the disk. For instance their data for ζ Tau are consistent with an extremely thin disk at an inclination of 74° or with a thicker disk viewed exactly edge on. In fact, our value for the opening angle of ζ Tau, i.e. 22°, which is half the value given by Waters et al. (1987), better agrees with the upper limit of 20° found by Quirrenbach et al. (1997) from a Gaussian fit to the Mk III interferometric measurements.

7. Measuring Be circumstellar envelopes with the VLTI

In the coming months, the MIDI instrument for the Very Large Telescopes Interferometer (VLTI) will provide the first IR measurements of the circumstellar disks at 10 μm and AMBER will perfom next year the first observations at 2 μm with an angular resolution of a few mas and a spectral resolution up to 10 000. Both instruments will allow a (u, v) plane coverage that will permit 2D analyses of Be disks with a detailled study of the kinematics within the disks thanks to the differential mode, i.e. following the photocenter displacement $\boldsymbol{\epsilon}(\lambda)$ as a function of wavelength (λ), see for instance Stee (1996) and Stee & Domiciano (2002) for more details. Thus the question of the disk thickness hopefully will be cleared up, especially for Be stars seen edge-on (i.e. without sin i ambiguity).

This study may help in the selection of the best targets since it appears that most of the Be stars, at least those in the Rinehart et al. (1999) sample, have wind densities between 10^{-13} and 10^{-12} g cm^{-3} for K magnitudes within 2 and 6. In Fig. 9 we have plotted visibilities for a 25 000 K, 10 $R_\odot$ Be star seen at 200 pc within the wind density range given in the previous section. It turns out that, for Be stars with a

Table 2. List of Be targets for the VLTI AMBER focal instrument with estimated visibilities, with a 60 m baseline, for the two hypotheses of the wind density, i.e. 10^{-13} and 10^{-12} g cm^{-3}.

VLTI Be Target list							
Name	RA (1950)	Dec (1950)	SpT	m_K	d (pc)	$V_{\max}$	$V_{\min}$
HD 10144	01 35 51.307	–57 29 24.92	B3Vpe	0.88	44.0	0.11	0.07
HD 37795	05 37 50.211	–34 05 58.71	B7IVe	2.84	82.2	0.22	0.14
HD 50013	06 47 58.321	–32 26 58.64	B1.5IVne	3.57	242.1	0.65	0.42
HD 56139	07 12 46.89	–26 41 05.0	B2IV-Ve	3.99	283.2	0.76	0.49
HD 58715	07 24 26.357	+08 23 29.89	B8Ve	3.04	52.2	0.14	0.09
HD 63462	07 46 00.39	–25 48 42.7	B1IV:nne	3.98	757.5	1.0	1.0
HD 89080	10 12 33.047	–69 47 21.33	B8IIIe	3.2	113.5	0.30	0.19
HD 91465	10 30 14.487	–61 25 39.66	B4Vne	3.05	152.4	0.41	0.26
HD 105382	12 05 29.23	–50 22 58.1	B6IIIe	4.8	115.2	0.31	0.20
HD 105435	12 05 45.445	–50 26 38.32	B2IVne	3.3	121.2	0.32	0.21
HD 112091	12 51 39.65	–56 53 51.0	B5Vne	5.6	110.7	0.29	0.19
HD 127972	14 32 19.305	–41 56 21.76	B1.5Vne	3.04	94.6	0.25	0.16
HD 135734	15 15 02.58	–47 41 33.4	B8Ve	4.3	89.1	0.24	0.15
HD 148184	16 24 07.29	–18 20 40.2	B2Vne	3.42	149.9	0.40	0.26
HD 158427	17 27 58.353	–49 50 19.59	B2Vne	3.8	74.3	0.20	0.13
HD 212571	22 22 43.381	+01 07 22.87	B1Ve	3.87	337.8	0.91	0.59

$V_{\max}$: Wind density $\rho_0 = 10^{-13}$ g cm^{-3}.
$V_{\min}$: Wind density $\rho_0 = 10^{-12}$ g cm^{-3}.

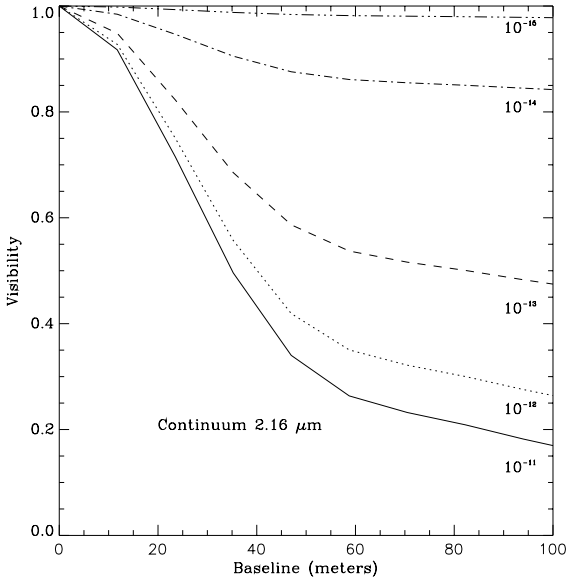

Fig. 9. Visibility curves for a 25 000 K, 10 $R_\odot$ radius Be star seen at 200 parsecs as a function of baseline (in meters) for different wind densities at the base of the photosphere (in g cm^{-3}).

K magnitude between 2 and 6, i.e. a density range between 10^{-12} and 10^{-13} g cm^{-3}, the disk must be very well resolved even with short baselines of the order of 40 meters. Nevertheless, the exact visibility will depend on the angle of inclination (sin i), the position of the envelope major axis projected into the sky plane compared to the projection of the interferometer baseline and of course, the distance of the star.

As already mentioned in the previous section, the effective temperature of the star is not a key parameter since the visibilities remain virtually unchanged for $T_{\rm eff}$ between 16 000 and 40 000 K (see Fig. 10). Thus, in order to obtain an estimation of the visibility of a Be star disk seen at a distance d (in parsec), with a wind density of 10^{-13} g cm^{-3} and a 60 m baseline one can use the relation given by:

$$V_{\max} = 2.7 \times 10^{-3} d_{\rm pc} \quad (10)$$

whereas for the same star but with a wind density of 10^{-12} g cm^{-3} the relation becomes:

$$V_{\min} = 1.75 \times 10^{-3} d_{\rm pc}. \quad (11)$$

Using Eqs. (10) and (11) it may be better to chose a larger or shorter interferometric baseline in order to better constrain the disk size of a given Be star knowing its distance in parsec.

On the other hand, a visibility measurement for a given baseline will give you an estimation of the wind density following Fig. 9. Thus, knowing the K magnitude it is also possible to estimate the disk opening angle and the mass loss of the star using the relationships plotted in Figs. 7 and 8.

In Table 2 we present the list of our Be targets proposed for the AMBER VLTI focal instrument with, for each star, the estimated visibilities for the two wind density hypothesis, i.e. 10^{-13} and 10^{-12} g cm^{-3}. It follows that except for HD 63462 all our 16 targets will be resolved with a 60 m baseline even for disks with a low density at the base of the stellar photosphere. It is

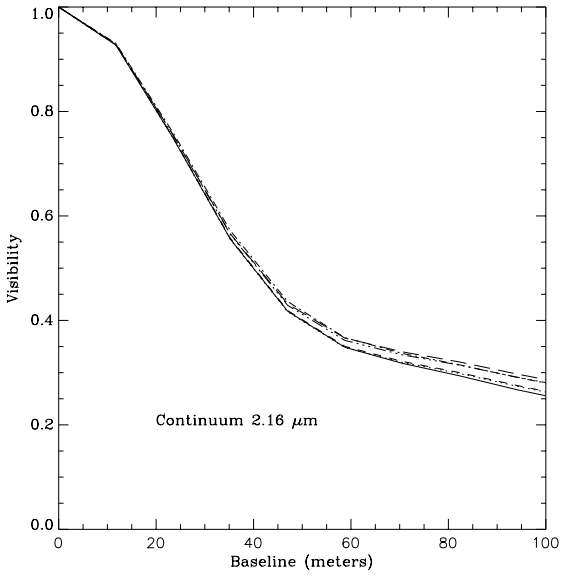

Fig. 10. Visibility curves for a 10 $R_\odot$ radius Be star seen at 200 parsecs with a wind densities at the base of the photosphere of 10^{-12} g cm^{-3}, as a function of baseline (in meters) for different effective temperatures, respectively 16 000, 20 000, 25 000, 30 000, 35 000 and 40 000 K. Since the differences are very small, the curves are superimposed.

also important to note that using differential interferometry we may use shorter baselines, especially for very well-resolved Be stars (for instance HD 10144 or HD 58715). This is mandatory since the relation between the phase of the visibility and the photocenter displacement remains valid as long as the source remains unresolved or "slightly" resolved.

Acknowledgements. The author thanks Armando Domiciano Jr and Nicolas Nardetto for careful reading of the manuscript and Eric Aristidi for his help in the choice of the Be stars given in the list of the VLTI targets. The distances given Table 2 are taken from the SIMBAD database.

References

Araújo, F. X., & Freitas Pacheco, J. A. 1989, MNRAS, 241, 543
Bjorman, J. E., & Cassinelli, J. P. 1993, ApJ, 409, 429
Castor, J. I., Abbott, D. C., & Klein, R. I. 1975, ApJ, 195, 157
Dachs, J., Engels, D., & Kiehling, R. 1988, A&A, 194, 167
Gehrz, R. D., Hackwell, J. A., & Jones, T. W. 1974, ApJ, 191, 675
Hony, S., Waters, L. B. F. M., Zaal, P. A., et al. 2000, A&A, 355, 187
Lamers, H. J. G. L. M., & Waters, L. B. M. 1987, A&A, 182, 80
Owocki, S. P., Cranmer, S. R., & Blondin, J. M. 1994, ApJ, 424, 887
Poe, C. H., & Friend, D. 1986, ApJ, 311, 317
Quirrenbach, A., Bjorkman, K. S., Bjorkman, J. E., et al. 1997, ApJ, 479, 477
Rinehart, S. A., Houck, J. R., & Smith, J. D. 1999, AJ, 118, 2974
Scuderi, S., Panagia, N., Stanghellini, C., et al. 1998, A&A, 332, 251
Stee, Ph., & Araújo, F. X. 1994, A&A, 292, 221
Stee, Ph., Araújo, F. X., Vakili, F., et al. 1995, A&A, 301, 219
Stee, Ph. 1996, A&A, 311, 945
Stee, Ph., Vakili, F., Bonneau, D., et al. 1998, A&A, 332, 268
Stee, Ph., & Bittar, J. 2001, SB, A&A, 367, 532
Stee, Ph., & Domiciano de Souza, A. Jr 2002, Science with differential phase, EuroWinter School Les Houches (EDP Sciences, EAS Publications Series), in press
Waters, L. B. F. M., Coté, J., & Lamers, H. J. G. L. M. 1987, A&A, 185, 206
Yudin, R. V. 2001, A&A, 368, 912